^{3}He(γ, d)^{1}H cross section from 10 to 21 MeV

C. C. Chang*
University of Maryland, Department of Physics, College Park, Maryland 20742

W. R. Dodge and J. J. Murphy, II†
National Bureau of Standards, Washington, D.C. 20234

(Received 27 August 1973)

A measurement of the ^{3}He(e,d)^{1}H 90° differential cross section between 10 and 21 MeV was made. The ^{3}He(e,d)^{1}H cross section was converted into a ^{3}He(γ,d)^{1}H cross section. The shape of the ^{3}He(γ,d)^{1}H cross section agrees with recent theoretical calculations. We find no evidence for the anomalies (structure) in the ^{3}He(γ,d)^{1}H 90° differential cross section at excitation energies of 14.5 and 19.5 MeV reported in two recent experiments.

[NUCLEAR REACTIONS ^{3}He(e,d), E_γ = 10–21 MeV; deduced $\sigma(E_\gamma, 90°)$.]

I. INTRODUCTION

Since the photon-absorption mechanism is largely model independent, the magnitude and average shape of the ^{3}He photodisintegration cross section provide information primarily about rescattering effects in the continuum states. On the other hand, structure in the ^{3}He cross section would be important because it could be most simply interpreted as providing evidence for the existence of excited states in the three-nucleon system. Two recent experiments have given evidence for such structure. The first anomaly or structure was reported by van der Woude, Halbert, Bingham, and Belt[1] (WHBB). The WHBB anomaly in the ^{3}He(γ, d)^{1}H cross section appeared to be a broad resonance at an excitation energy of 19.5 ± 0.5 MeV. The second anomaly was reported by Chang, Diener, and Ventura[2] (CDV) and occurred at an excitation energy of 14.5 ± 0.5 MeV and had a width of 2 MeV. CDV noted that previous electro- and photodisintegration experiments did not show this anomaly. We show below that because of the kinematic smearing inherent in the use of a high initial electron bombarding energy relative to the excitation energy the previous electrodisintegration experiments[3] in which only the deuteron was detected did not have sufficiently small experimental errors to resolve the anomaly seen by CDV. We have measured the 90° differential cross section in the excitation energy interval of 10 to 21 MeV with sufficiently low electron bombarding energies and sufficiently small errors so that both the WHBB and CDV anomalies would have been observable.

Our measurements of the ^{3}He(e, d)^{1}H cross section are consistent with a structureless, smooth cross section and do not reproduce the anomalies seen in the experiments of either WHBB or CDV. Our absolute cross section is fitted in shape and to within 11% in magnitude by the theoretical calculation of Barbour and Phillips[4] (BP) in which the final state is described by a wave function which is the solution of the Faddeev equations in the separable approximation and by a recent refinement of the BP calculation by Lehman and Gibson[5] (LG).

II. ELECTRODISINTEGRATION EXPERIMENTS

The similarity between reactions induced by fast charged particles and those induced by incident electromagnetic waves has long been known and often exploited.[6,7] Here we derive the formulas used to relate our ^{3}He(e, d)^{1}H experimental yields to the ^{3}He(γ, d)^{1}H cross section and investigate the differences between ^{3}He photo- and electrodisingegration experiments which arise from an undetected electron of finite momentum in the final state of the ^{3}He(e, d)^{1}H reaction. We use the Møller potential $A_\mu(\omega, \vec{q})$ to describe the electron's transition electromagnetic field as it transits from an initial energy and momentum $(k, \vec{K})$ to a final energy and momentum $(k', \vec{K}')$ while transferring energy and momentum $(\omega, \vec{q})$ to a nucleus of energy and momentum $(E_A, \vec{P}_A)$. This nucleus disintegrates into a particle with energy and momentum $(E, \vec{P})$ and a residual nucleus of energy and momentum $(E_{A-P}, \vec{P}_{A-P})$. The transition matrix element is

$$\langle H(\vec{q})\rangle = A_\mu(\omega, \vec{q}) J_\mu(\omega, \vec{q}), \tag{1}$$

where

$$A_\mu(\omega, \vec{q}) = -e \frac{u(\vec{K}')\gamma_\mu u(\vec{K})}{q^2 - \omega^2}, \tag{2}$$

$u(\vec{K}')$ and $u(\vec{K})$ are the final and initial state electron spinors, γ_μ is the μth component of the usual Dirac matrices, and $J_\mu(\omega, \vec{q})$ is the matrix element of the current operator multiplied by $e^{-i(\vec{q}\cdot\vec{r}-\omega t)}$ evaluated between initial and final nuclear states. Here $\vec{r}$ and t refer to the coordinate space of the nuclear system. Conservation of the nuclear transition current and the Lorentz condition for the Møller potential can be used to reduce the transition matrix element to

$$\langle H(\vec{q})\rangle = \vec{A}\cdot\vec{J} - (\vec{q}\cdot\vec{A})(\vec{q}\cdot\vec{J})/\omega^2 . \tag{3}$$

To emphasize the similarities between electro- and photodisintegration we decompose the nuclear current into components perpendicular (transverse) and parallel (longitudinal) to the momentum transfer $\vec{q}$ (i.e., $\vec{J} = \vec{J}_t + \vec{J}_l$). Since $\vec{J}_l = \vec{q}(\vec{q}\cdot\vec{J})/q^2$,

$$\langle H(\vec{q})\rangle = \vec{A}\cdot[\vec{J}_t + (1 - q^2/\omega^2)\vec{J}_l] = \vec{A}\cdot\vec{m} = \vec{A}\cdot(\vec{m}_t + \vec{m}_l) , \tag{4}$$

where $\vec{m}_t = \vec{J}_t$ and $\vec{m}_l = (1 - q^2/\omega^2)\vec{J}_l$. The differential electrodisintegration cross section per incident electron is

$$d^6\sigma_e = \frac{2\pi}{v_e}\delta(k + E_A - k' - E_{A-P} - E)\frac{1}{2(2j_i+1)} \times\sum |\langle H(\vec{q})\rangle|^2 \rho_{e'}\rho_P . \tag{5}$$

Here v_e is proportional to the relative flux per incident electron and $\rho_{e'}$ and ρ_P are the densities of final electron and nucleon states, and the sum is over the initial- and final-state electron spins and the initial and final nuclear states. If we abbreviate $u(\vec{K}')\vec{\gamma}u(\vec{K})$ by $\vec{\Gamma}$, Eq. (5) can be written[6]

$$d^6\sigma_e = \frac{2\pi}{v_e}\delta(\omega + E_A - E_{A-P} - E)\frac{4\pi\alpha}{(q^2-\omega^2)^2} \times\frac{m_e^2}{kk'}\frac{1}{2(2j_i+1)}\sum|\vec{\Gamma}\cdot\vec{m}|^2\frac{d^3\vec{K}'}{(2\pi)^3}\frac{d^3\vec{P}}{(2\pi)^3} , \tag{6}$$

where α is the fine structure constant and m_e is the electron mass. The photodisintegration cross section is given by

$$d^3\sigma_\gamma = 2\pi\delta(\omega_\gamma + E_A - E_{A-P} - E)\frac{1}{2(2j_i+1)} \times\frac{1}{2\omega_\gamma}\sum|m_t|^2\frac{d^3\vec{P}}{(2\pi)^3} . \tag{7}$$

The sum in Eq. (7) is over the two polarization states of the photon and over the initial and final nuclear states. The yield of particles produced by a bremsstrahlung spectrum $I(\omega_\gamma)d\omega_\gamma/\omega_\gamma$ photons per energy interval $d\omega_\gamma$ is

$$2\pi\delta(\omega_\gamma + E_A - E_{A-P} - E)\frac{I(\omega_\gamma)d\omega_\gamma}{\omega_\gamma}\frac{1}{2(2j_i+1)} \times\frac{1}{2\omega_\gamma}\sum|m_t|^2\frac{d^3\vec{P}}{(2\pi)^3} . \tag{8}$$

The similarity between Eq. (6) and Eq. (8) emphasizes the close relationship which exists between electro- and photodisintegration.[6] If we let

$$I_e = m_e^2\sum|\vec{\Gamma}\cdot\vec{m}|^2 , \tag{9}$$

then after performing the sum and average over final and initial electron spins and using $K'^2 = K^2 + q^2 - 2Kq\cos\theta_q$, where θ_q is the angle between $\vec{K}$ and $\vec{q}$,

$$I_e = \sum\{2|\vec{K}\cdot\vec{m}_t|^2 + \tfrac{1}{2}(q^2-\omega^2)|\vec{m}_t|^2 + (\vec{K}\cdot\vec{m}_t^*\vec{m}\cdot\vec{q} + \vec{K}\cdot\vec{m}_t\vec{m}^*\cdot\vec{q})(K^2-K'^2)/q^2 + \tfrac{1}{2}[-\omega^2 + (K^2-K'^2)^2/q^2]|\vec{m}_l|^2\} . \tag{10}$$

Expressions for $\vec{J}$ in terms of a multipole expansion in the c.m. system of the virtual photon and the target nucleus have been given by Pratt, Walecka, and Griffy.[8] For an electric dipole transition

$$\vec{J} = \sum_\lambda J_\lambda \vec{e}_{q\lambda} , \tag{11a}$$

where

$$J_\lambda = i(\pi)^{1/2}\langle f|\vec{J}_{op}\cdot[(2)^{1/2}j_2(qr)\vec{Y}^\lambda_{121}(\theta_r,\varphi_r) - 2j_0(qr)\vec{Y}^\lambda_{101}(\theta_r,\varphi_r)] + (6)^{1/2}q^2 j_1(qr)\vec{Y}^\lambda_{111}(\theta_r,\varphi_r)\cdot\vec{\mu}(\vec{r})|i\rangle . \tag{11b}$$

In the expressions above $\vec{e}_{q\lambda}$ are spherical unit vectors defined with respect to a rectangular coordinate system as $\vec{e}_{q1} = -(2)^{-1/2}(\vec{e}_x + i\vec{e}_y)$, $\vec{e}_{q-1} = (2)^{-1/2}(\vec{e}_x - i\vec{e}_y)$, and $\vec{e}_{q0} = \vec{q}/q$, $\vec{J}_{op}$ is the convection current operator, $\vec{\mu}(\vec{r})$ is the magnetization operator, $j_0(qr)$ and $j_2(qr)$ are the usual spherical Bessel functions, and $\vec{Y}^\lambda_{101}(\theta_r,\varphi_r)$ and $\vec{Y}^\lambda_{121}(\theta_r,\varphi_r)$ are vector spherical harmonics. In the long-wavelength approximation

$$\vec{J}^{E1} = \langle f|J_x\vec{e}_x + J_y\vec{e}_y + J_z\vec{q}/q|i\rangle . \tag{11c}$$

Hence, $\vec{m}_t$ and $\vec{m}_l$ are vectors of the form

$$\vec{m}_t = M_t^{E1}(\omega, q)[(\vec{q}\times\vec{P})\times\vec{q}]/Pq^2 \tag{11d}$$

and

$$\vec{m}_l = M_l^{E1}(\omega, q)[(q^2-\omega^2)/\omega^2](\vec{q}\cdot\vec{P})\vec{q}/Pq^2, \tag{11e}$$

since the final-state wave function can be expanded in terms of eigenstates of the total angular momentum and since the initial state is an S state. We have assumed $\vec{q}\cdot\vec{r} \ll 1$, and in this approximation $M_t^{E1}(\omega, q) = M_l^{E1}(\omega, q) = M^{E1}(\omega)$, but we shall maintain the distinction between M_t^{E1} and M_l^{E1} in order to make explicit the contributions from transverse and longitudinal momentum transfers. Substituting Eqs. (11d) and (11e) into Eq. (10),

$$\begin{aligned} I_e = \sum \{ & 2K^2 \sin^2\theta_P \sin^2\theta_q \cos^2\varphi |M_t|^2 + \tfrac{1}{2}(q^2-\omega^2)\sin^2\theta_P |M_t|^2 \\ & - 2(K/q)[(q^2-\omega^2)/\omega^2](K^2-K'^2)\sin\theta_P \cos\theta_P \sin\theta_q \cos\varphi \,\mathrm{Re}(M_t M_l) \\ & + \tfrac{1}{2}[(q^2-\omega^2)/\omega^2]^2[-\omega^2 + (K^2-K'^2)^2/q^2]\cos^2\theta_P |M_l|^2\}, \end{aligned} \tag{12}$$

since $(\vec{q}\times\vec{P})\cdot(\vec{q}\times\vec{K}) = q^2PK\sin\theta_P \sin\theta_q \cos\varphi$, where θ_P is the angle between $\vec{q}$ and $\vec{P}$, θ_q is the angle between $\vec{q}$ and $\vec{K}$, and φ is the angle between the $(\vec{q}, \vec{P})$ and $(\vec{q}, \vec{K})$ planes. In an electrodisintegration experiment in the context used here, the scattered electron is not detected in coincidence with the emitted particle and hence the vector $\vec{q}$ is not determined. Furthermore, the virtual photon energy ω is given to first order in $(m_e/k')^2$ by

$$\omega = \omega_\gamma \left[1 - \frac{q_0^2 - \omega_0^2}{\omega_0 M_A}\left(1 - \frac{1}{2}\frac{\omega_0}{M_A}\right)\right], \tag{13a}$$

where

$$\omega_\gamma = \omega_{\gamma 0}/(1 + 2\omega_{\gamma 0}/M_A)^{1/2}, \tag{13b}$$

$$\omega_{\gamma 0} = \left[\frac{M_A T_P + S(M_A - M_P + \frac{1}{2}S)}{M_A - M_P - T_P + P\cos\theta_{P'}}\right]_0, \tag{13c}$$

$$\omega_0 = \omega_{\gamma 0}\frac{1 + (k_0/\omega_{\gamma 0})\tau}{1+\tau}, \tag{13d}$$

and

$$\tau = \left[\frac{P(\cos\theta_{e'P} - \cos\theta_{P'}) + 2K\sin^2(\frac{1}{2}\theta_{e'e})}{M_A - M_P - T_P + P\cos\theta_{P'}}\right]_0. \tag{13e}$$

Here $\theta_{P'}$ and $\theta_{e'P}$ are the angles between the initial and scattered electron and the detected particle, $\theta_{e'e}$ is the angle between the incident and scattered electron, M_A and M_P are the masses of the target nucleus and the emitted particle, respectively, and S is the two-body separation energy. The subscript 0 indicates that all variables to the left are to be evaluated in the laboratory system. The virtual and real photon energies in the c.m. system of the virtual and real photon and the target nucleus are ω and ω_γ. Note that Eqs. (13) will limit the phase space available to the scattered electron in certain kinematic situations.

In deriving the usual expressions for virtual photon intensity spectra, the nuclear matrix elements M_t and M_l are evaluated at $\omega = \omega_\gamma$. This approximation is valid if the nuclear matrix elements M_t and M_l are slowly varying over the region in which the factors multiplying M_t and M_l in Eq. (12) divided by $(q^2-\omega^2)^2$ become small compared to their value at $\omega = \omega_\gamma$ or if ω is independent of the direction of the scattered electron. The latter condition is equivalent to $\tau k_0/\omega_{\gamma 0} \ll 1$. If either of the above conditions is satisfied, the electrodisintegration cross section can be integrated over scattered electron directions without the assumption of a nuclear model to give the dependence of M_t and M_l on ω. Explicitly,

$$d^3\sigma_e = \frac{\alpha}{2\pi}\frac{1}{K^2}\frac{1}{2(2j_i+1)}\int \frac{2KK' I_e d\Omega_{e'}}{(q^2-\omega^2)^2}\frac{d^3\vec{P}}{(2\pi)^3}. \tag{14}$$

Since the momentum of the incident electron and the emitted particle are the quantities observed in the laboratory, we evaluate Eq. (14) in a coordinate system in which $\vec{K}$ is in the direction of the z axis. The relationship between $\vec{K}$, $\vec{K}'$, $\vec{q}$, and $\vec{P}$ is shown in Fig. 1.

After integration over $\varphi_{e'e}$

$$\begin{aligned} \int I_e d\varphi_{e'e} = 2\pi \sum \{ & 2K^2 \sin^2\theta_q [\tfrac{1}{2}\sin^2\theta_{P'} + \sin^2\theta_q P_2(\cos\theta_{P'})]|M_t|^2 + \tfrac{1}{2}(q^2-\omega^2)[\sin^2\theta_{P'} + \sin^2\theta_q P_2(\cos\theta_{P'})]|M_t|^2 \\ & - (K/q)[(q^2-\omega^2)/\omega^2](K^2-K'^2)\sin\theta_q \sin 2\theta_q P_2(\cos\theta_{P'})\,\mathrm{Re}(M_t M_l) \\ & + \tfrac{1}{2}[(q^2-\omega^2)/\omega^2]^2[-\omega^2 + (K^2-K'^2)^2/q^2][\cos^2\theta_{P'} - \sin^2\theta_q P_2(\cos\theta_{P'})]|M_l|^2\}, \end{aligned} \tag{15}$$

where $\theta_{P'}$ is the angle which $\vec{P}$ makes with $\vec{K}$. Integration over $\varphi_{e'e}$ is roughly equivalent to a polarization average in photodisintegration.[6] Using $\sin^2\theta_q = [(K+K')^2 - q^2][q^2 - (K-K')^2]/4K^2q^2$, the integration over $\theta_{e'e}$

can be converted into an integration over dq^2. Finally, the $E1$ electrodisintegration cross section in the approximation stated above is given by

$$d^3\sigma_e = \frac{\alpha}{\omega^2}\frac{1}{2(2j_i+1)}\sum\Big(\{[2R_{k'}\eta - \tfrac{1}{2}(1+R_{k'})^2\delta - R_{k'}]\sin^2\theta_{P'} - [\tfrac{1}{2}R_\omega^2(1+R_{k'})^2\delta - R_{k'}(1+R_{k'}^2)]P_2(\cos\theta_{P'})\}|M_t|^2$$
$$+R_\omega^2\{\eta\sin^2\theta_{P'} + \tfrac{1}{2}[\tfrac{1}{2}(1+R_{k'})^2\delta - R_{k'}]P_2(\cos\theta_{P'})\}|M_t|^2$$
$$-2R_{k'}R_\omega(1+R_{k'})[\tfrac{1}{2}(1+R_{k'})\delta + R_{k'}/R_\omega]P_2(\cos\theta_{P'})\,\mathrm{Re}(M_tM_l)\{[(1+R_{k'})^2\delta - 2R_{k'}]\cos^2\theta_{P'}$$
$$-\tfrac{1}{2}[\tfrac{1}{2}(1+R_{k'})^2(3-2R_{k'}+3R_{k'}^2)\delta - R_{k'}(3+4R_{k'}+3R_{k'}^2)]P_2(\cos\theta_{P'})\}|M_l|^2\Big)\frac{d^3\vec{P}}{(2\pi)^3}\,, \quad (16)$$

where $R_{k'}=k'/k$, $R_\omega=\omega/k$, $\eta=\ln[(kk'+KK'-m_e^2)/m_e\omega]$, $\delta=\ln[(k+k')/\omega]$. Equation (16) is correct to order $(m_e/k')^2$ and all quantities are evaluated in the c.m. system of the virtual photon and target nucleus. Equation (16) shows explicitly the contributions from momentum transfers transverse and longitudinal to the average direction of $\vec{q}$. Since $M_t=M_l$ in the long-wavelength approximation

$$d^3\sigma_e = 2\frac{\alpha}{\omega}\{[(1+R_{k'}^2)\eta - 2R_{k'} - \tfrac{3}{2}R_{k'}^2]\sin^2\theta_{P'} + R_{k'}^2\}\frac{1}{2(2j_i+1)}\frac{1}{2\omega}\sum|M_t|^2\frac{d^3\vec{P}}{(2\pi)^3}\,. \quad (17)$$

Comparison of Eq. (17) with Eq. (8) shows the quantity

$$N_e^{E1}(k,\omega) = \frac{\alpha}{\pi}\{[(1+R_{k'}^2)\eta - 2R_{k'} - \tfrac{3}{2}R_{k'}^2]\sin^2\theta_{P'} + R_{k'}^2\} \quad (18)$$

may be associated with the spectrum of virtual photons and is roughly equivalent in this context to $I(\omega_\gamma)$ for the real photon bremsstrahlung spectrum.

The initial and final electron energies, and the virtual photon energy in the c.m. system of the virtual photon and the target nucleus, (k, k', and ω), are related to the same quantities (k_0, k_0', and ω_0) measured in the laboratory by $(M_Ak_0 - \frac{1}{2}q_\mu^2)/W$, $(M_Ak_0' + \frac{1}{2}q_\mu^2)/W$, and Eq. (13a), where W and q_μ^2 are the Lorentz invariants $[(M_A+\omega_0)^2 - q_0^2]^{1/2}$ and $(q_0^2-\omega_0^2)$. Numerical integration of Eq. (14) shows that 95% of the contributions to Eq. (18) arise from electrons scattered through angles less than those given by $\theta_{e'e\,95\%} \approx 22 - 104R_{k'} + 120R_{k'}^2$. Under the conditions of our experiment, the differences between evaluating N^{E1} using k, k', and ω evaluated at $\theta_{e'e}=0$ or $\theta_{e'e95\%}<2\%$.

The ^{3}He(e, d)^{1}H experiment of Kundu, Shin, and Wait[3] used an incident electron bombarding energy of 86 MeV and hence the conditions which validate Eq. (18) were not satisfied. To obtain an estimate of the shape of the electrodisintegration cross section we make a model-dependent calculation using as our model the CDV photodisintegration cross section, $\sigma_\gamma^{\mathrm{CDV}}$. We assume

$$M_t^2 = 12\pi\omega\sigma_\gamma^{\mathrm{CDV}} \quad (19)$$

and $M_t=M_l$. Outside the range of the CDV cross section appropriate extrapolations of the cross section were used to represent M_t. These values of M_t were inserted into Eq. (14) and the integral over $d\Omega_{e'}$ converted into an integration over $d(\cos\theta_{e'e})$ and $d\omega$ by means of a Jacobian transformation. If we denote the model-dependent estimate of σ_e by σ_e^M, then

$$d^3\sigma_e^M = \int S(k,\omega)\sigma_\gamma^{\mathrm{CDV}}(\omega)d\omega\frac{d^3\vec{P}}{(2\pi)^3}\,, \quad (20a)$$

where

$$S(k,\omega) = \frac{\alpha}{4\pi}\frac{1}{k}\int\frac{k'I_e}{(q^2-\omega^2)^2}\frac{1}{|M_t|^2}\frac{\partial\varphi_{e'e}}{\partial\omega}\,d(\cos\theta_{e'e}); \quad (20b)$$

$\partial\varphi_{e'e}/\partial\omega$ was obtained from Eqs. (13) and

$$\cos\theta_{e'd} = \cos\theta_{e'e}\cos\theta_{ed} + \sin\theta_{e'e}\sin\theta_{ed}\cos\varphi_{e'e'}. \quad (20c)$$

Figure 2 shows the normalized excitation energy distribution function or smearing function $S(k,\omega)/N_e^{E1}(k,\omega)$ evaluated for $\omega=14$ MeV and $k=22$ and 90 MeV. Hence, the yield of deuterons observed at fixed deuteron momentum were produced by a

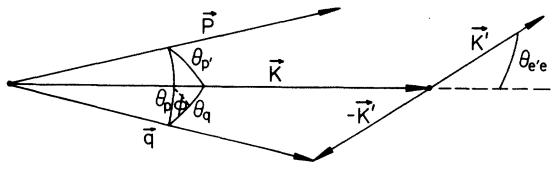

FIG. 1. Relationship between the momentum of the incident electron $\vec{K}$, the scattered electron $\vec{K}'$, and the momentum transfer $\vec{q}$. The momentum of the emitted particle $\vec{P}$, and the angles $\theta_{e'e}$, θ_q, θ_P, $\theta_{P'}$, and ϕ defined in the text are also shown.

band of excitation energies centered around a mean excitation energy which is close to that of the photodisintegration experiment. The curves in Fig. 3 are the result of evaluating Eq. (20a) for various incident electron energies.

III. EXPERIMENTAL RESULTS

We measured the ^{3}He$(e, d)^1$H cross section at the National Bureau of Standards linear electron accelerator facility with a magnetic spectrometer and data-logging apparatus described previously.[9] We made three 24-h runs. Two of these 24-h runs were made with target cell walls of 0.53 mg/cm^2 of Mylar and average ^{3}He pressures of 0.37 atm. In the other 24-h run these quantities were 0.76 mg/cm^2 and 0.70 atm, respectively. The ^{3}He gas was assayed after the completion of each run and found to contain less than 0.13% air. The incident electron energies were 21 and 23 MeV.

Our differential electrodisintegration cross section is defined by

$$\left(\frac{d\sigma}{d\Omega}\right)_{\text{lab}} = \frac{C_d}{n_t \Delta\Omega N(k, \omega) d\omega/\omega}\ , \tag{21}$$

where C_d is the number of deuterons of total energy E_d, average kinetic energy T_d, and momentum P_d recorded by a focal plane counter of momentum acceptance interval $\Delta P_d/P_d$ per incident electron. The spectrometer solid angle is $\Delta\Omega$ and n_t is the number of ^{3}He nuclei/cm^2 in a distance equal to the average width of the trapezoidally shaped magnet transmission function. $N(k, \omega)/\omega$ is the number of real and virtual photons in the excitation energy interval $d\omega$. The excitation energy interval $d\omega$ is related to the deuteron energy acceptance interval of the spectrometer dT_d, by

$$d\omega = \frac{d\omega}{dT_d}\left[\left(\frac{dT_d}{dx}\right)_i \Big/ \left(\frac{dT_d}{dx}\right)_m\right]_{^3\text{He}} \times \left[\left(\frac{dT_d}{dx}\right)_m \Big/ \left(\frac{dT_d}{dx}\right)_f\right]_{\text{Mylar}} dT_d'. \tag{22}$$

The quantities $(dT_d/dx)_{i,m,f}$ refer to the deuteron energy loss/unit length in the ^{3}He gas and Mylar window evaluated at the kinetic energy the deuteron had at the center of the gas cell (i), at the ^{3}He-Mylar window interface (m), and the energy (momentum) measured by the spectrometer magnet (f).[10] These factors correct for the dilation of dT_d' due to energy loss as the deuteron leaves the target. The quantity $d\omega/dT_d'$ can be obtained from Eq. (13) and the virtual photon contribution to $N(k, \omega)$ can be obtained from Eq. (18). The virtual photon energy was calculated using Eq. (13) assuming forward electron scattering. In all cases (10 MeV $< \omega <$ 20 MeV) the difference between this estimate of ω and the median value of ω was <20 keV for k = 21 MeV.

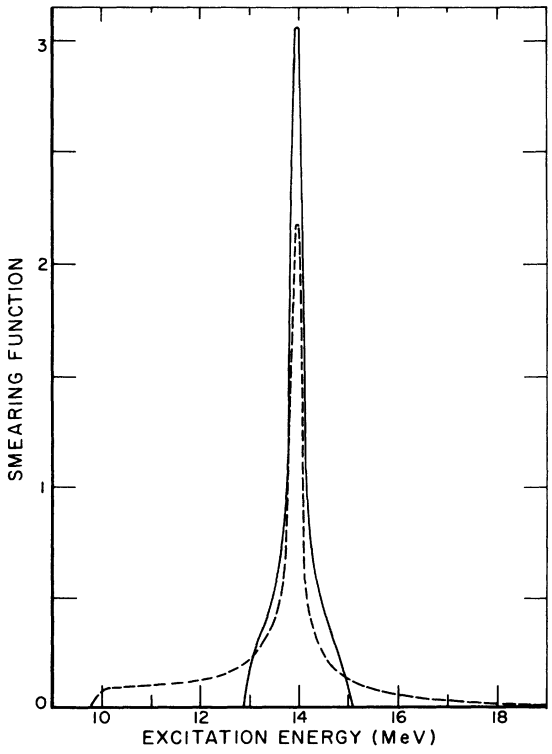

FIG. 2. Excitation energy distribution function for the excitation energies producting deuterons of 2.806 MeV at 90° in the laboratory. The solid curve is for an incident electron energy of 22 MeV, the dashed curve for an incident electron energy of 90 MeV. The curve for a disintegration induced by a real photon would be a δ function at 14 MeV.

Our center-of-mass 90° differential cross section is shown in Fig. 4. The data were taken at a laboratory angle of 90° and were converted to 90° in the center-of-mass system by assuming that $(d\sigma/d\Omega)_{\text{c.m.}} = b \sin^2\theta(1 - \frac{1}{2}\beta\cos\theta)^2$. Values of β were taken from Barbour and Hendry.[11] Numerical values of the cross section are given in Table I. The errors are only statistical. Table II summarizes the errors contributing to the uncertainties in our absolute cross section. We verified the dependence of $N_e^{E1}(k, \omega)$ on k by measuring the electroproduction yields from ^{2}H at fixed proton energy as a function of k. The relative counting efficiencies of our 150-μm-thick surface-barrier focal plane counters were deduced by measuring the counting rate of a ^{210}Po α source placed inside a target cell pressurized with CF_4 as a function of CF_4 pressure.[12] The counting rate was independent of pressure

over a range of pressures corresponding to α energies from 1 to 5.3 MeV. From these data we conclude that our deuteron counting efficiencies were 100% for deuteron energies of interest here. Also shown in Fig. 4 are the data of CDV converted to the ^{3}He$(e, d)^1$H reaction. The difficulty which CDV had in extracting areas (photon counts) from pulse-height spectra by photon-line shape fitting led them to arbitrarily assign errors to their data considerably larger than the usual counting statistics and may have been responsible, in part, for the occurrence of the CDV anomaly. CDV estimate the error in the absolute cross section to be ±20%.

In Fig. 5 we have plotted our data, and the radiative capture data of van der Woude *et al.* (WHBB),[1] and of Halbert, Paul, Snover, and Warburton (HPSW).[13] WHBB used a novel method of measuring the ^{3}He$(\gamma, d)^1$H cross section by measuring the ^{1}H$(d, h)\gamma$ cross section with a magnetic spectrometer. These data gave evidence for a resonance in the ^{3}He$(\gamma, d)^1$H cross section at an excitation energy of 19.5 MeV. To check these data HPSW measured the ^{2}H$(p, \gamma)^3$He differential cross section at 90° and found no evidence for a resonance between 15 and 22.5 MeV. The difficulties which WHBB had with their experiment were thought by Halbert to be confined to excitation energies above ≈16 MeV. Above ≈16 MeV the (d, h) reaction on ^{12}C, ^{13}C, and target impurities, particularly ^{16}O, in WHBB's polystyrene (CH) target constituted a copious and apparently intractable source of background. The data of WHBB have an absolute calibration of ±7% and the HPSW data have been normalized to the WHBB data below 16 MeV. The slight difference in slope between our data and the data of HPSW may arise from a variation in photon detector efficiency with photon energy (estimated by HPSW to be 10–15%) which was not made to the HPSW data.[13] The agreement between our data, the HPSW data, and the truncated data of WHBB is satisfactory.

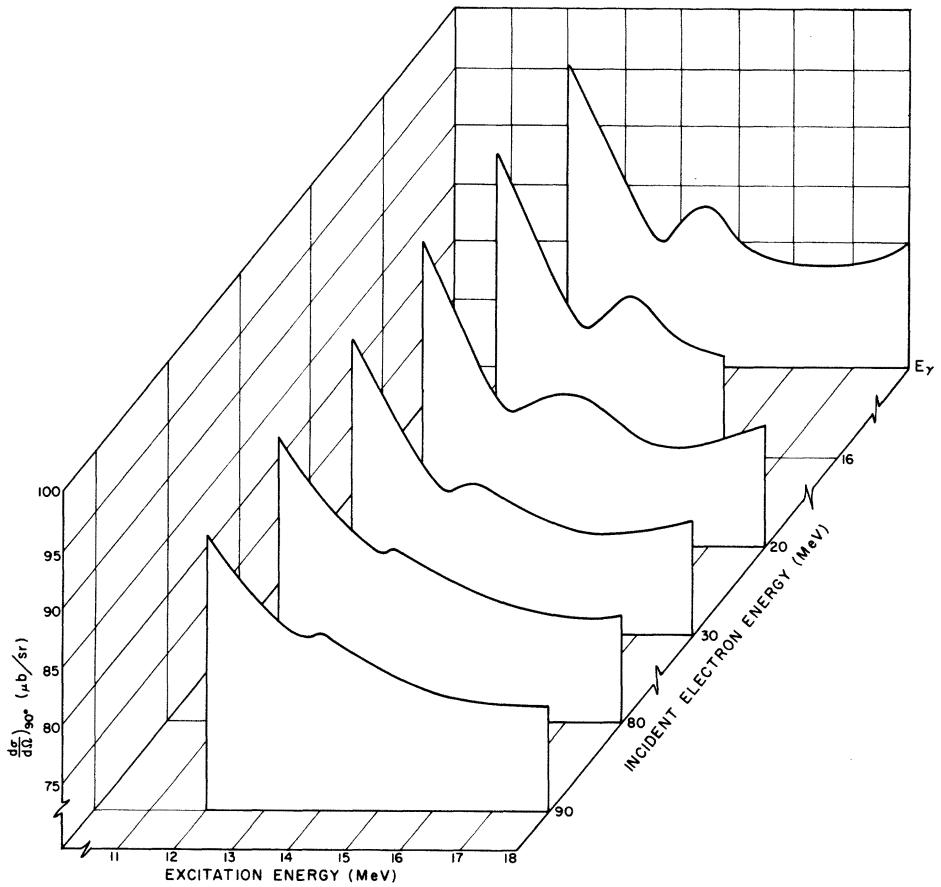

FIG. 3. Results of the conversion of the Chang, Diener, and Ventura (Ref. 2) photodisintegration cross section to electrodisintegration. The curve labeled E_γ is the ^{3}He$(\gamma, d)^1$H result of Chang, Diener, and Ventura (Ref. 2). The other curves are ^{3}He$(e, d)^1$H cross sections obtained by folding the CDV cross section with the excitation energy distribution function. Note that with increasing incident electron energy the structure becomes less pronounced.

The solid curve of Figs. 4 and 5 is the result of a calculation by Lehman and Gibson.[5] It is a refinement of a Faddeev type of calculation by Barbour and Phillips[4] which utilized S-wave separable spin-dependent potentials. The LG curve was calculated using the same input parameters as BP's normalized S-state wave function I (dashed curve of Fig. 4). LG first solved for the Nd off-shell amplitude and then expressed the $E1$ amplitude as a Born term plus an integral over the off-shell Nd amplitude times the off-shell $E1$ Born amplitude with the appropriate propagator inserted between them.

The curves in Fig. 6 show the effects of using ^{3}He wave functions which correspond to deuteron D-state probability densities of 0, 4, and 7%. These curves were taken from Hendry and Phillips (HP)[14] and include a correction for Coulomb repulsion in the proton-deuteron state which decreased the peak cross section in each case by about 7%.

TABLE I. Data from this experiment. All data are given in the center-of-mass system. Uncertainties are only counting statistics.

Excitation energy (MeV)	$(d\sigma/d\Omega)_{90°}$ [a] (μb/sr)
9.891	98 ± 6
10.266	104 ± 5
10.641	102 ± 4
11.016	111 ± 3
11.391	108 ± 4
11.766	120 ± 5
12.516	108 ± 4
12.891	102 ± 2
13.266	96 ± 2
13.641	96 ± 3
14.016	93 ± 2
14.391	90 ± 2
14.766	89 ± 2
15.141	86 ± 2
15.516	83 ± 2
15.891	80 ± 2
16.641	74 ± 3
17.016	73 ± 3
17.391	73 ± 3
17.766	65 ± 3
18.141	67 ± 3
18.516	60 ± 7
18.891	68 ± 5
19.266	66 ± 4
19.641	59 ± 5
20.016	52 ± 8
20.391	57 ± 8
20.766	47 ± 9

[a] The data were taken at a laboratory angle of 90° and were converted to 90° in the center-of-mass system by assuming $(d\sigma/d\Omega)_{c.m.} = b \sin^2\theta (1 - \frac{1}{2}\beta \cos\theta)^2$. Values of β were taken from Ref. 11. See also Ref. 1.

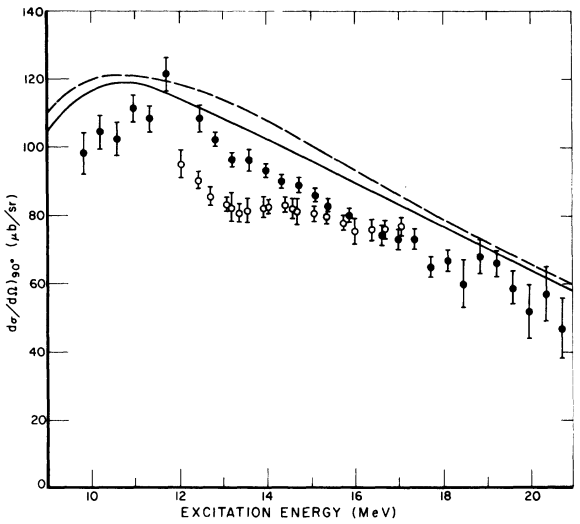

FIG. 4. The ^{3}He$(e,d)^1$H cross section as a function of excitation energy. The ● are the results of the current work; ○ the ^{3}He$(\gamma,d)^1$H results of Chang, Diener, and Ventura (Ref. 2) converted to the ^{3}He$(e,d)^1$H reaction as explained in the text. The solid curve is the calculation of Lehman and Gibson (Ref. 5), the dashed curve that of Barbour and Phillips (Ref. 4). All cross sections are absolute. The indicated uncertainties on our results include only counting statistics.

Although the calculations of LG and HP have no free parameters, we have computed the renormalization or scale factors which minimize the χ^2 fit of these calculations to the data. These factors are 0.87 for the theory of LG and 0.94, 1.07, and 1.21 for the theories of HP with 0, 4, and 7% D-state probabilities. While the magnitude of the HP cross section computed with 0 and 4% D-state probabilities averaged over the energy range of the data are in better agreement with this experiment than the LG cross section, the renormalized LG

TABLE II. Estimated uncertainties in $(d\sigma/d\Omega)$ exclusive of counting statistics.

Item	Uncertainties in %
I. Incident electron beam current	±2
II. Number of target nuclei	
(a) Target effective length	±2
(b) Target temperature	+3
(c) Target purity	+0.1
III. Miscellaneous	
(a) Spectrometer solid angle	±3.5
(b) Upper limit to real photon contamination from unknown sources	+2
(c) Shape of virtual photon spectrum	±2.5
$\left[\sum (\text{errors})^2\right]^{1/2}$	+6, −5

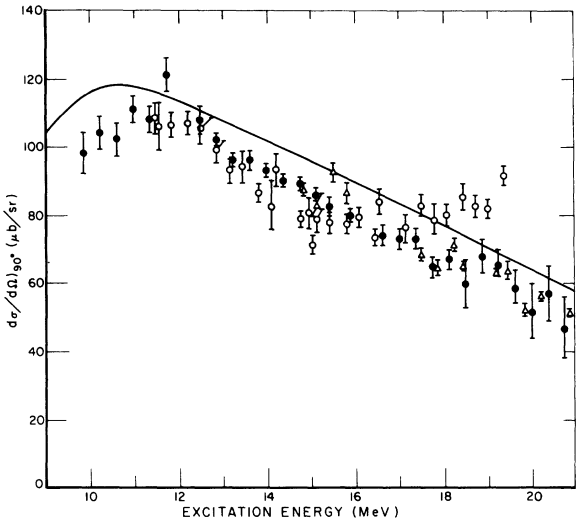

FIG. 5. ^{3}He two-body disintegration cross sections as a function of excitation energy. The ● are the results of the current work; ○ are the ^{1}H(d,^{3}He)γ data of van der Woude *et al.* (Ref. 1) converted to the ^{3}He(γ,d)^{1}H cross section by detailed balance showing the anomaly at 19 MeV; △ are the ^{2}H(p,γ)^{3}He data of Halbert *et al.* (Ref. 13). Note that the newer capture data of Halbert *et al.* (Ref. 13) as well as the ^{3}He(e,d)^{1}H data show no evidence for the rise seen in the data of van der Woude *et al.* (Ref. 1). The solid curve is the theoretical calculation of Lehman and Gibson (Ref. 5).

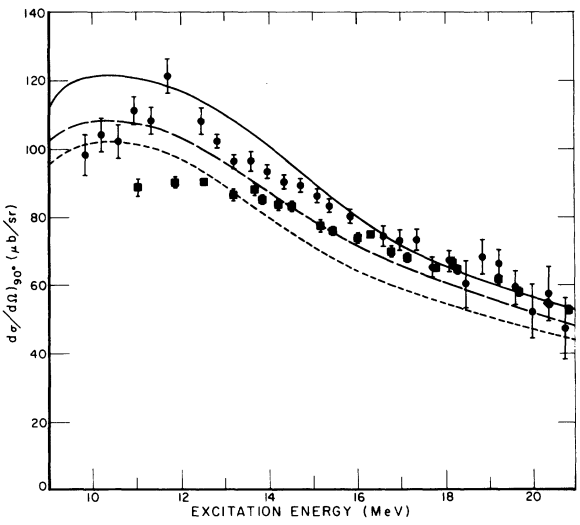

FIG. 6. The ^{3}He(γ,d) $E1$ 90° differential cross section calculated by Hendry and Phillips (Ref. 14) using Yamaguchi interactions which give 0% (solid curve), 4% (dashed curve), and 7% (dot-dashed curve) for the deuteron D-state probabilities. The ● are the results of the current work. The ■ are the ^{3}He(γ,d) data of Ticcioni *et al.* (Ref. 15).

cross section provides the best fit to the data, indicating that the LG theory has the more correct shape. Also shown in Fig. 6 are the data of Ticcioni *et al.*[15] which are in good agreement with the older data of Stewart, Morrison, and O'Connell[16] and Berman, Koester, and Smith.[17] The data of Ticcioni *et al.*.[15] Stewart, Morrison, and O'Connell,[16] and Berman, Koester, and Smith[17] are in good agreement with our data at 20 MeV but diverge from our data at lower energies until the disagreement becomes 15% at 11 MeV. We note that the correction we made to the deuteron energy interval in the gas target [Eq. (22)] was 2% at 20 MeV and 13% at 10 MeV.

IV. CONCLUSION

We conclude that our ^{3}He(e,d)^{1}H 90° differential cross section is in good agreement with the shape of the Barbour and Phillips[4] and Lehman and Gibson[5] calculations and in fair agreement (within 11%) with their absolute magnitude. Calculations by Hendry and Phillips,[14] which were made with ^{3}He wave functions containing 0 and 4% deuteron D-state probabilities and which included a correction for Coulomb repulsion in the proton-deuteron state, agree with our data within 6 and −7% in mean magnitude, but do not agree in shape. Our experiment is consistent with a structureless, monotonically decreasing cross section and hence corroborates neither in the experiment of CDV nor of WHBB with respect to the existence of structure in the ^{3}He(γ,d)^{1}H cross section.

ACKNOWLEDGMENTS

We wish to thank Dr. D. R. Lehman and Dr. E. G. Fuller for several helpful discussions. One of us (C. C. C.) wishes to acknowledge the hospitality of the Center for Radiation Research (Nuclear Sciences Division) at the National Bureau of Standards. The help of the National Bureau of Standards linac crew is gratefully acknowledged.

*Guest worker at the National Bureau of Standards.
†National Research Council Fellow, now at the Electron Accelerator Laboratory, University of Saskatchewan, Saskatoon, Saskatchewan, Canada.

[1] A. van der Woude, M. L. Halbert, C. R. Bingham, and B. D. Belt, Phys. Rev. Lett. 26, 909 (1971).
[2] C. C. Chang, E. M. Diener, and E. Ventura, Phys. Rev. Lett. 29, 307 (1972).

[3]S. K. Kundu, Y. M. Shin, and G. D. Wait, Nucl. Phys. A171, 384 (1971); D. M. Skopik and Y. M. Shin, Can. J. Phys. 50, 392 (1972).
[4]I. M. Barbour and A. C. Phillips, Phys. Rev. C 1, 165 (1970).
[5]D. R. Lehman and B. F. Gibson, private communication.
[6]R. H. Dalitz and D. R. Yennie, Phys. Rev. 105, 1598 (1957); J. M. Eisenberg, Phys. Rev. 132, 2243 (1963); B. Bosco and S. Fubini, Nuovo Cimento 9, 350 (1958); B. Bosco and P. Quarati, *ibid.* 33, 527 (1964).
[7]W. R. Dodge and W. C. Barber, Phys. Rev. 127, 1746 (1962).
[8]R. H. Pratt, J. D. Walecka, and T. A. Griffy, Nucl. Phys. 64, 667 (1965).
[9]D. M. Skopik and W. R. Dodge, Phys. Rev. C 6, 43 (1972).
[10]Energy loss data were obtained from L. C. Northcliffe and R. F. Schilling, Nucl. Data A7, 223 (1970).
[11]I. M. Barbour and J. A. Hendry, Phys. Lett. 38B, 151 (1972).
[12]W. R. Dodge and J. J. Murphy, II, Phys. Rev. Lett. 28, 839 (1972).
[13]M. L. Halbert, P. Paul, K. A. Snover, and E. K. Warburton, in *Proceedings of the International Conference on Few Particle Problems in Nuclear Physics, Los Angeles, California, 1972* edited by I. Šlaus, S. A. Moskowski, R. P. Haddock, and W. T. H. van Oers (North-Holland, Amsterdam, 1973).
[14]J. A. Hendry and A. C. Phillips, Nucl. Phys. A211, 533 (1973).
[15]G. Ticcioni, S. N. Gardner, J. L. Matthews and R. O. Owens, Phys. Lett. (to be published).
[16]J. R. Stewart, R. C. Morrison, and J. S. O'Connell, Phys. Rev. 138, B372 (1965).
[17]B. L. Berman, L. J. Koester, Jr., and J. H. Smith, Phys. Rev. 133, B117 (1964).